MRS Communications (2015), *5*, 115–129
doi:10.1557/mrc.2015.20

MRS Communications

Polymers/Soft Matter Prospective Article

Ferroelectric polymers as multifunctional electroactive materials: recent advances, potential, and challenges

Xiaoshi Qian, Shan Wu, Eugene Furman, and **Q.M. Zhang,** Department of Electrical Engineering and Materials Research Institute, The Pennsylvania State University, University Park, Pennsylvania 16802, USA
Ji Su, NASA Langley Research Center, Hampton, Virginia 23681, USA

Address all correspondence Xiaoshi Qian, Q. M. Zhang at **xyq5004@psu.edu; qxz1@psu.edu**

(Received 23 February 2015; accepted 14 April 2015)

Abstract

As multifunctional electroactive materials, ferroelectric polymers are unique owing to their exceptionally high dielectric strength (>600 MV/m), high flexibility, and easy and low-temperature fabrication into required shapes. Although polyvinylidene difluoride (PVDF)-based ferroelectric polymers have been known for several decades, recent findings reveal the potential of this class of electroactive polymers (EAPs) to achieve giant electroactive responses by tuning the molecular, nano, and meso-structures. This paper presents these advances, including giant electrocaloric effect, giant electroactuation, and large, hysteresis-free polarization response. New developments in materials benefit applications, such as environmentally benign and potentially highly energy-efficient electrical field controlled solid-state refrigeration, artificial muscles, and high-energy and power density electric energy storage devices. The challenges in developing these materials to realize these applications, and strategies to further improve the responses of EAPs will be also discussed.

Introduction

Ferroelectricity was first observed in inorganics (Rochelle salt) by Valasek in 1920.[1] After the humble beginnings extending approximately to the World War II, when only a handful of ferroelectrics were known, there was an explosion of new materials and applications first in inorganic and later polymeric materials. Interests in these materials have not abated, and several major areas of their usage are outlined in this paper which emphasizes recent developments in ferroelectric polymers for energy storage, cooling, and artificial muscles.

The intrinsic symmetry of the ferroelectric material enables not only ferroelectricity, which is associated with a spontaneous electric polarization in a material that can be switched by an electric field, but also coexisting piezoelectricity and pyroelectricity, which are the electro-mechanical energy conversion and electro-thermal energy conversion processes, respectively, as is illustrated in Fig. 1(a). Ferroelectricity in polymers was discovered much later in 1970s in the polyvinylidene difluoride (PVDF) homopolymer and later in PVDF-based copolymers such as P(VDF–TrFE) [TrFE, (trifluoroethylene)].[2] These multifunctional electroactive polymers (EAPs),[3] which are flexible and lightweight, and can be easily processed into different shapes by room temperature (RT) or low-temperature fabrication methods, have attracted a great deal of public attention and been employed and investigated for a broad range of applications, including strain/stress sensors, transducers for ship navigations (Sonar) and medical imaging, infrared (IR)-sensors, energy harvesting, and high-density memory devices, just to name a few.[4–12] Figure 1(b) depicts the unit-cell structures of PVDF α- and β-phases (the ferroelectric phase).[13] Figure 1(c) is the polarization hysteresis loop from the P(VDF–TrFE) 65/35 mol% copolymer.

Our daily experiences have taught us that polymers can withstand large strains without breaking (tuber band). Besides a high spontaneous polarization [see Fig. 1(c), where $P_s > 0.1$ C/m^2], ferroelectric polymers also intrinsically have a high dielectric strength (dielectric breakdown fields >600 MV/m). As will be shown in this paper, these features can be utilized to develop PVDF-based ferroelectric polymers, by modifying the molecular and nanostructures, that: (i) exhibit giant electrocaloric effect (ECE), i.e., an electric field-induced temperature change of more than 30 °C in bulk materials.[14–16] A few years ago, no-one would image that applying an electric pulse can induce appreciable cooling in polymers, which we observed recently by properly engineering the nano- and meso-polarization coupling in the ferroelectric PVDF-based polymers. (ii) Generate electrostrictive strains more than order of magnitude higher than in ferroelectric ceramics. The capability of large shape change induced electrically in certain classes of EAPs, mimicking the biological muscles, has gained them the name of "artificial muscles".[17] And (iii) ultra-high electric energy storage density capability with fast charge/discharge speed, thus attractive for applications such as in hybrid electric

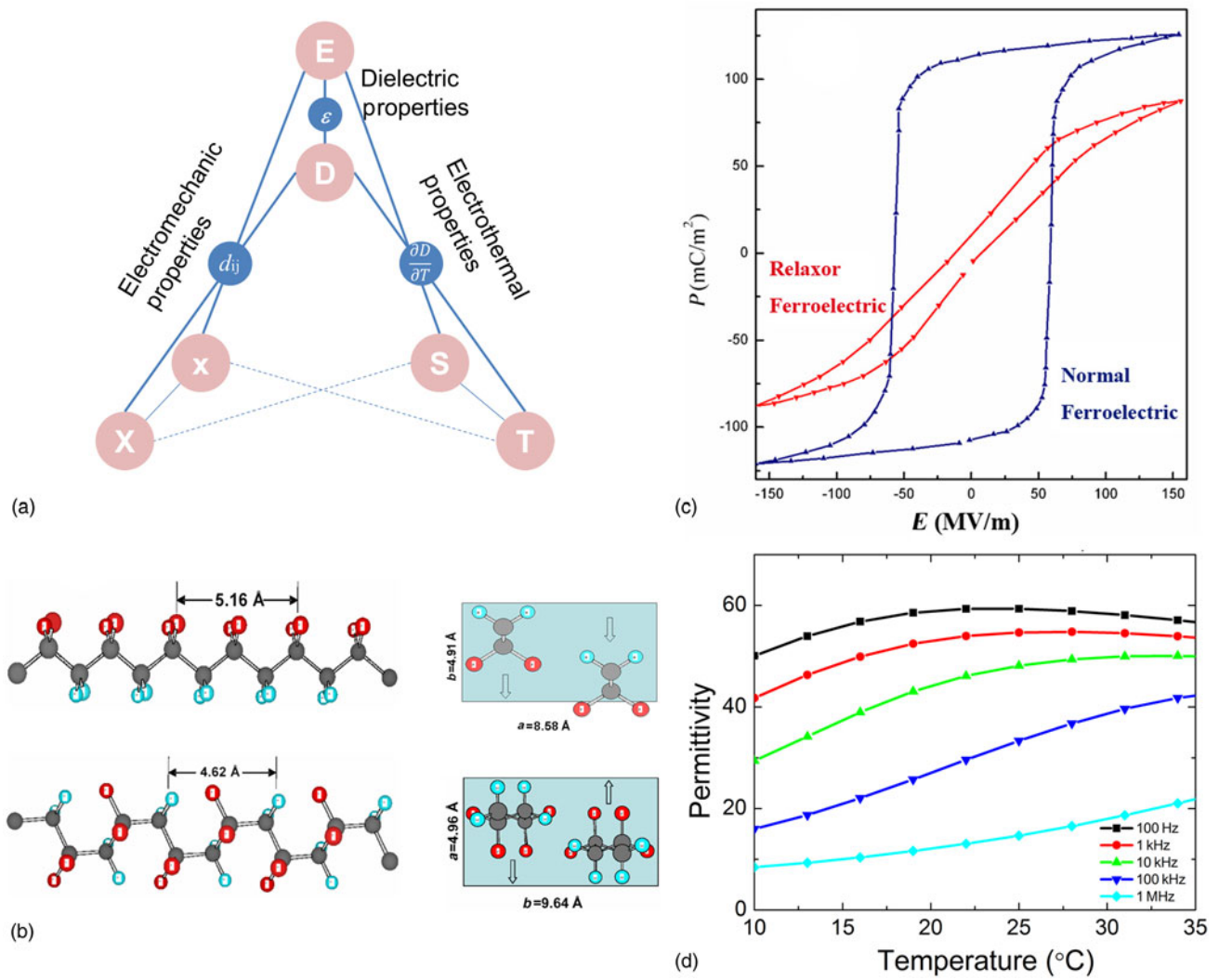

Figure 1. (a) A schematic illustrating the multifunctional couplings in the ferroelectric EAPs. (b) Schematic illustration of unit-cell structures of α- and β-phases of PVDF. (c) D-E loops for P(VDF-TrFE) (blue lines) and P(VDF-TrFE–CFE) (red lines) measured at 10 Hz. (d) Dielectric constant (permittivity) of P(VDF-TrFE-CFE) versus temperature and frequency.

vehicles (HEV), medical deliberators, pulse-forming networks, and switching-mode power supplies.[18–21]

These multifunctional EAPs in which more than one property can be tuned by electric signals are particularly interesting considering the fact that they can be easily fabricated, making use of the three-dimensional (3D) printing technology, into different shapes in a single material system that contains many functionalities to meet the ever increasing demand for flexible, wearable, highly mobile, and biocompatible compact electroactive devices.

Giant ECE in modified ferroelectric PVDF-based polymers

The pyroelectric effect and ECE are related through Maxwell's equations for the ferroelectric PVDF-based polymers. Although the pyroelectric effect,

$$p = \left(\frac{\partial G}{\partial T}\right)_{\mathrm{E}} \tag{1}$$

has been widely studied for PVDF-based ferroelectric polymers because of their potential applications for IR-sensors, the very small ECE, <1 °C electric field-induced temperature change, renders them not attractive for practical cooling devices. In 2004, based on the Landau–Devonshire theoretical analysis, Zhang et al. predicted a large ECE in ferroelectric PVDF-based polymers.[22] The free energy G of a ferroelectric material in the thermodynamic Landau–Devonshire theory in stress-free condition,[2]

$$G = G_0 + 1/2\,a\,P^2 + 1/4\,b\,P^4 + 1/6\,c\,P^6 - EP, \tag{2}$$

where G_0 is the free energy of the non-ferroelectric phase, P is the polarization, and E is the electric field. For most normal

ferroelectrics, $a = \beta(T - T_c)$, where b, c, β, and T_c are constants. From $\Delta S = -(\partial G/\partial T)_E$, the isothermal entropy change ΔS due to the spontaneous polarization change is

$$\Delta S = -1/2\,\beta P^2. \tag{3}$$

From $\Delta Q = C_E \Delta T = T\Delta S$, the adiabatic temperature change is

$$\Delta T = 1/2\ T\beta P^2/c_E, \tag{4}$$

where c_E is the specific heat. For the P(VDF–TrFE) 65/35 mol% ferroelectric polymers, relevant parameters are $\beta = 3.5 \times 10^7$ J/mK/C^2, $P = 0.1$ C/m^2, yielding a $\Delta S = -96$ J/kg K. Taking the FE–PE transition of 100 °C and the specific heat of $c_E = 1.4 \times 10^3$ J/kg K, $\Delta T = 26$ °C is estimated. This estimation suggests a giant ECE in ferroelectric PVDF-based polymers when operating near the FE–PE transition. Moreover, based on the Maxwell equation,

$$\left(\frac{\partial S}{\partial E}\right)_T = \left(\frac{\partial P}{\partial T}\right)_E. \tag{5}$$

Zhang et al. further suggested in 2004 that the relaxor ferroelectric polymers, may also exhibit a giant ECE near RT.[22]

These predictions have been verified by a series experiments starting from 2008.[14,23–33] As presented in Fig. 2(a), an electric field-induced temperature change of nearly 30 °C has been obtained in the P(VDF–TrFE) 65/35 mol% copolymer, modified by high-energy electron irradiation.[34] In addition, the giant ECE exhibits a unique temperature-independent behavior across a useful temperature range spanning the RT in Fig. 2(b).[23,34]

Figure 3(a) illustrated the general principle of ECE in a dipolar material, which shows that the ECE is determined by the dipolar state entropy differences between the dipolar-ordered phases under respective electric fields,

$$\Delta T = \frac{T}{C_E}[S_p(0, T) - S_p(E, T)], \tag{6}$$

where $S_p(0,T)$ is the dipolar entropy when $E = 0$, and $S_p(E,T)$ corresponds to the entropy of a dipole-aligned state when E is applied. Pirc et al. derived the saturation ΔT in a dipolar material[35]:

$$\Delta T_{sat} = \frac{T \ln \Omega}{3\varepsilon_0 \Theta C} P_S^2 \tag{7}$$

where P_s is the saturation polarization, Ω is the configuration number (number of polar entities), C is the specific heat, ε_0 is the vacuum permittivity and Θ is the effective Curie constant. Therefore, the development of polar-dielectrics with a large Ω as well as a small Θ is highly desirable, especially if P_s can be kept unchanged. In relaxor ferroelectrics, breaking of translational symmetry by defect modification of periodic lattice can lead to a larger numbers of local states and hence may increase Ω compared with its normal ferroelectric counterpart. In ferroelectrics, Θ is directly related to the polar-correlation length and the presence of random defect-mediated fields. In particular, relaxor ferroelectrics have much smaller polar regions compared with normal ferroelectrics. These considerations suggest that relaxor and highly disordered ferroelectrics may exhibit larger ECE than conventional ferroelectrics. Besides large ECE, defect modulation de-stabilizes ferroelectric phase thus the ferroelectric–paraelectric (FE-PE) transition induced large ECE can be achieved in a much wider temperature range as shown in Fig. 2(b). For a P(VDF–TrFE–CFE) 59.2/33.6/7.2 mol%, relaxor ferroelectric terpolymer, the ECE response is nearly temperature independent from 0 to 45 °C,

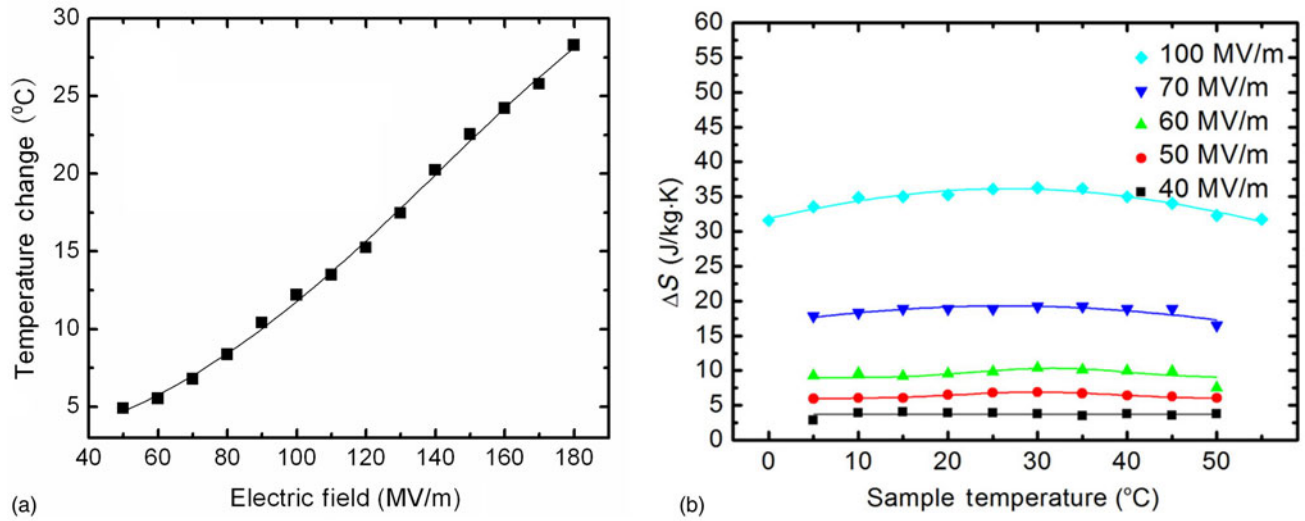

Figure 2. EC performances in defect-modulated ferroelectric polymer. (a) EC temperature drop is reaching 27 K under $\Delta E = 180$ MV/m, in irradiated ferroelectric polymer P(VDF–TrFE) 65/35. (b) EC performance in P(VDF–TrFE–CFE) shows temperature-independent behavior.

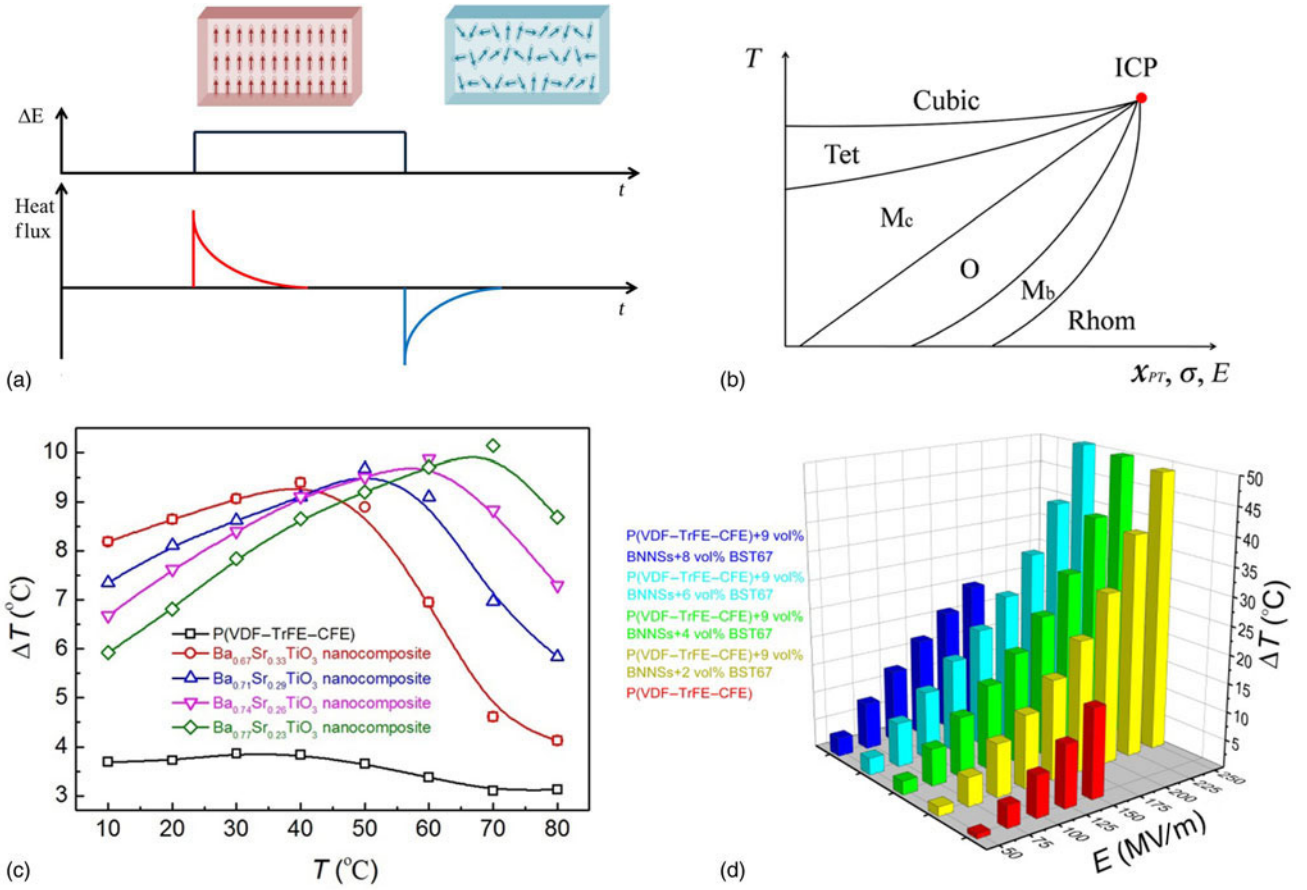

Figure 3. (a) A schematic illustration of dipolar ordered to disordered transition that is electrically tunable. (b) ICP that brings multiphases as coexistence states. Reprinted with permission from Ref. 37. Copyright [2012], AIP Publishing LLC (c) ΔT of nanocomposites (BST as the nanofilers) under 75 MV/m and comparison with the terpolymer matrix, (d) ΔT of nanocomposites under different electric fields and comparison with the terpolymer. Adapted with permission from Ref. 41, Copyright (c) [2015] John Wiley and Sons Inc.

which is in sharp contrast to that in normal ferroelectrics where ECE peaks at the FE–PE transition and displays strong temperature dependence.[32,36] Such temperature independent ECE is attractive for practical cooling device applications. These results reveal the intricate roles played by the defects in tailoring the ferroelectric response and its nano-polar domains to generate large ECE and its temperature dependence.

As shown in Eq. (7), the dipolar entropy is a function of the number of polar entities, $S \propto \ln(\Omega)$. One approach to significantly increase the number of polar entities, as suggested by a recent theoretical study by Liu et al., is to operate the ferroelectric material near an invariant critical point where multiphases [more than two phases, as illustrated in Fig. 3(b)] coexist (in contrast to the two phases coexistence near the normal critical point).[37] Correlated experimental demonstration has been reported in inorganic material near the invariant critical point (ICP) where both ECE and EC coefficients were markedly improved.[38,39] In PVDF-based polymers, besides the ferroelectric β-phase, there are also other phases reported such as α-, γ, and δ phases, as well as the so-called the low-temperature phase for P(VDF–TrFE) copolymers at compositions below 65/35 mol%. How to design molecular, nano-, and meso-structures to realize the multiphases coexistence and a possible ICP will be an interesting research direction to pursue.

Polymer nanocomposites, which mix two or more types of dissimilar materials, offer the possibility in achieving states with larger number of coexisting phases and near-ICP ECE behavior. Moreover, the interfacial regions could generate additional ECE through interfacial effects, i.e., the total entropy change ΔS of a biphasic composite (with two different materials) is

$$\Delta S = f_1 \Delta S_1 + (1 - f_1) \Delta S_2 + \Delta S_{intf}, \quad (8)$$

where f_1 is the volume fraction of the first constituent and ΔS_{intf} represents the contribution from the interface. In fact, nanocomposites have significantly expanded capabilities and functionalities far beyond these achievable in single component materials.[40] Recently Zhang et al. reported a ternary nanocomposites containing P(VDF–TrFE–CFE) (62.3/29.9/7.8 mol%) as

polymer matrix, $Ba_{0.67}Sr_{0.33}TiO_3$ (BST67) as active EC ceramic nanofiller which has FE transition at 27 °C, and boron nitride nanosheets, to enhance ECE, breakdown strength E_b and thermal conductivity.[41] As shown in Figs. 3(c) and 3(d), the ternary nanocomposite with enhanced material properties is expected to reach higher cooling power density (27 W/cm^3) owing to higher allowable operating frequency of the cooling devices, as shown in the finite-element simulation of a simple heat pump with regeneration process.[42,43] Interestingly, mixtures of relaxor P(VDF–TrFE–CFE) and ferroelectric P(VDF–TrFE) also exhibit strong modulation in ECE and E_b. When the concentration of ferroelectric phase is small (<10 wt%), the blends will be dominated by the terpolymer thus the blends show large ECE at RT. In addition, interfaces between random relaxor and ordered ferroelectric phases generate additional polarization contribution, which contributes to ECE as it is indeed observed in those blends at RT.[44,45]

To design a refrigerator with continuing cooling capability, people realized early on that EC refrigerator should be designed as a heat pump.[46–55] Regeneration processes are commonly used in EC cooling devices to improve the device's performance. Both fluid and solid regenerators have been employed to facilitate thermal energy harvesting and cooling.[56–58] Sinyavsky and Brodyansky[51] demonstrated a $T_{span} = 5$ K ($T_{span} = T_h - T_c$, where T_h and T_c are the hot and cold ends temperature, respectively) across a 55 mm EC refrigerator which was about twice of ΔT (the adiabatic temperature change) of the EC material. Gu et al. reported that by employing a solid plate with anisotropic thermal conductivity as a regenerator, an EC polymer-based cooling device with a T_{span} of more than 6 K was demonstrated across a 20 mm long EC refrigerator with about 2.5 K adiabatic temperature change of the EC element.[47,48]

Although external regenerators have been widely utilized in refrigerator designs in both magnetocaloric and electrocaloric (EC) coolers, the irreversible heat loss introduced by the external regenerators dramatically reduces device performances. More recently, an EC cooler without external regenerator was proposed to reach higher cooling power and efficiency.[43] The self-regenerative cooling device is operating with two rings contacting each other and rotating in opposite directions, as shown in Fig. 4(a). With effective regenerative process, temperature span T_{span} between the hot end and cold end of a cooling device can be effectively widened compared with the EC temperature drop of the EC material solely [Fig. 4(b)]. Wide operating temperature span T_{span} is highly desired for practical cooling devices. To evaluate the refrigerating performance of a heat pump, cooling power, and coefficient of performance (COP) are considered as two key parameters, former for cooling capability and later for efficiency, respectively. High cooling power requires large EC response, including ΔS and ΔT, and high operating frequency. The COP is defined as $COP = Q_C/W$, where Q_C is the energy absorbed as the cold end of the device and W is the input work.

There are many challenges in realizing practical EC refrigeration, including further improving EC polymer's performance.

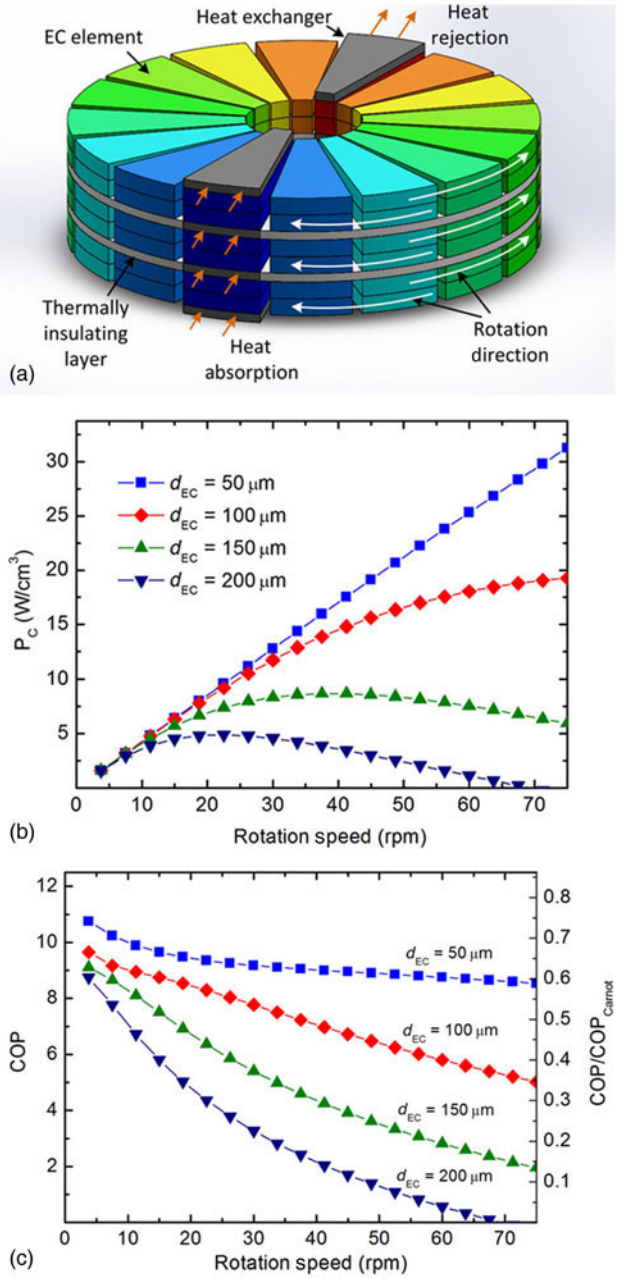

Figure 4. (a) A schematic illustration of a solid state EC cooler, which exhibits a high cooling power density and COP. The self-regenerative operation contains two rings of EC modules rotating in opposite directions. (b) The numerical simulation result of the performances of the EC cooler with different EC module thickness. The material properties of EC modules are chosen from EC polymer P(VDF–TrFE–CFE). Reprinted with permission from Ref. 43. Copyright [2014], AIP Publishing LLC.

Dielectric loss, which is shown as the hysteresis loop area in D–E loops, generates excessive heat that may dramatically reduce the COP of the EC refrigerator. How to enhance dipolar entropy change without simultaneously inducing additional dielectric loss remains a challenge. As one would normally find, P(VDF–TrFE–CFE) exhibits larger ECE, but it also shows larger double hysteresis

loops compared with P[VDF–TrFE–chlorotrifluoroethylene (CTFE), which exhibits smaller ECE, but with the slimmer hysteresis.[59] Larger dipolar response, which is needed for generating large ECE, is at the cost of losing pinning effect of chemical bonds, causing broader hysteresis loops. In addition, for certain applications, such as biomedical and on-chip cooling, small voltage is desirable because of the safety and reliability issues. Enhancement of ECE at lower field, such as 50–80 MV/m is thus highly desired. Several approaches may be employed to address above considerations. Stretching a RFE polymer may enhance the crystallinity and promote ordering in a zero-field scenario. It has been proved that at high field (100 MV/m), the stretching would cause ECE to behave in a more temperature-dependent manor. However, at relatively lower field (50 MV/m), the ECE is expected to be larger in stretched films compared with non-stretched ones. The enhancement may originate from the partially ordered zero-field state which behaves as if the film been subjected to an internal field that would effectively improve the low-field performance of ECE. Introducing multi-caloric effect may also enhance the ECE. It has been reported theoretically that, by utilizing an external strain, ECE can be strongly enhanced.[60] On the other hand, ECE improvement should not be limited to pursuing larger effect. Since ECE is a reversible temperature/entropy change under electric field, the nature of ECE limits the ECE-based refrigeration to heat pump operation. It is very interesting to ask whether ECE polymer can cool under an electric pulse without generating any subsequent heating. For certain application such as on-chip hotspot cooling and potential biomedical applications, such instant cooling capability is highly demanded.[61,62] Hence, how to design the ferroelectric polymer structure in various scales to achieve such instant cooling would be an interesting research field with significant value for both academia and industry.

Electromechanical coupling in PVDF-based ferroelectric polymers

Among all electroactive responses, ferroelectric polymers have long been sought for use as artificial muscles, which would exhibit a large shape change induced electrically. PVDF homopolymer and its copolymer P(VDF–TrFE), owing to large electronegativity differences for constituent species and suitable atomic size, exhibit large dipole moment (2 Debye per unit cell) in all-trans conformations known as β-phase,[63,64] leading to a ferroelectric phase that can be characterized by ferroelectric hysteresis loop as shown in Fig. 1(c). In the ferroelectric phase, applying an electric field induces a polarization change and correspondingly, the piezoelectric response. It is apparent that the small piezoelectric strain, which is about 0.1% even under 100 MV/m electric field, is too small to be practical for artificial muscles, not to mention many other applications where large electroactuations, which are orders of magnitude higher than the piezoelectric strain, are desired. The electrostriction associated with a large polarization change in the ferroelectric polymers may provide a solution to this challenge. As an example, Fig. 1(b) compares the crystal structures of the α-, which has trans-gauche (TGTG') bonds, and β-, which has all-trans bonds, phases. In phase transformation between the α- and β-phases, besides a polarization change, there is also the possibility of a large accompanying strain, due to the large differences in the unit-cell dimensions. This is the molecular origin of the large electrostriction in these ferroelectric polymers. The ferroelectric phase of PVDF-based polymers has the β-crystal structure and the paraelectric phase that can be regarded as a mixture of TGTG′ molecular conformation and TG_3TG_3' molecular conformation. Hence one would expect a large strain generated as the polymer transitions between the FE and PE phases, which was indeed observed. The implication of this observation is that by applying an electric field to induce a FE–PE transition (on the PE phase side), a large electroactuation (~10% strain) could be achieved in PVDF-based polymers when measured along the polymer chain direction. An electrostrictive strain associated with FE–PE transition is limited near the transition temperature that is normally away from RT. How to achieve the large strain effect at a wider temperature span and covering the RT is therefore important for many practical applications. In late 1990s and early 2000s, Zhang et al. showed that by defects modification,[65–78] nano-sized polar domain can be formed in the ferroelectric polymer to convert the material into a relaxor ferroelectric, as seen in Fig. 1(c) which is a near hysteresis-free polarization loop at RT measured from a relaxor ferroelectric P(VDF–TrFE–CFE) terpolymer. These relaxor ferroelectric polymers exhibit a large electrostriction [see Fig. 5(a)]. There are typically two approaches to introduce defects into the ferroelectric P(VDF–TrFE) copolymer to convert it into a relaxor ferroelectric: (i) Irradiation of the copolymer with high-energy electrons or

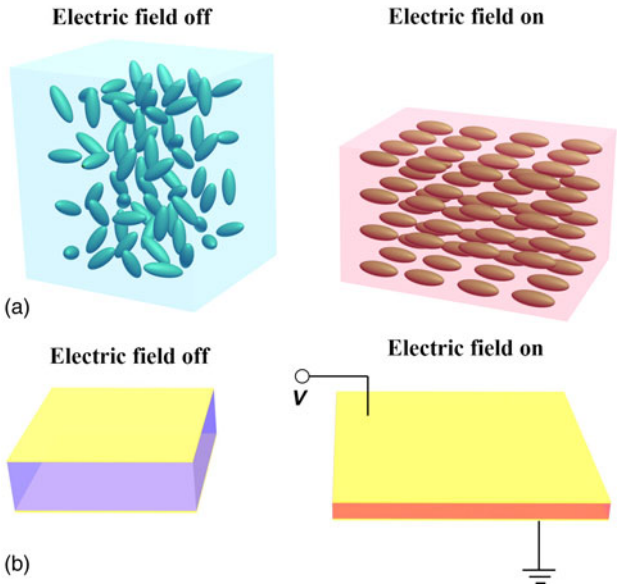

Figure 5. Schematics illustration of (a) electrostriction and (b) Maxwell stress effect.

protons.[65–68] (ii) Copolymerizing the polymer with a third monomer which is bulkier than VDF and TrFE, such as chlorofluoroethylene (CFE), chlorotrifluoroethylene (CTFE), or hexafluoropropylene (HFP).[65,69–71,76–80] The high-energy irradiation or additional bulky monomer in the ferroelectric P(VDF–TrFE) reduces the size of polar-domains which destabilizes the ferroelectric phase and stabilizes a more disordered phase covering a much wider temperature range of useful strain actuation. As a result, relaxor ferroelectric polymers exhibit very little ferroelectric hysteresis [Fig. 1(c)] and high dielectric constant covering RT, as shown in Fig. 1(d).

In general, the electrostriction, which exists in all dielectrics, originates from the rearrangement or creation of dipoles with respect to the external electric field. As was well summarized by Cheng et al., strains induced by electrostriction are related to the electric polarization as[17]:

$$x = QP^2 = Q\varepsilon_0^2(\kappa - 1)^2E^2, \quad (9)$$

where x is the strain, Q is the electrostrictive coefficient, P is the polarization, ε_0 is the vacuum permittivity, and κ is the relative permittivity. In Eq. (9), we assumed that the ferroelectric polymer is a linear dielectric, for the sake of comparison with the Maxwell stress-induced actuation, which will be discussed later. The large electrostrictive strain (>5% along the polymer chain direction) plus the high elastic modulus (~500 MPa) generate a high elastic energy density, which is a measure of the strain and stress generation capability of an actuator material.

A two end-supported unimorph diaphragm actuator utilizing electrostrictive polymer has been developed capable of a displacement of nearly 50 μm [see Fig. 6(a)].[81] The diaphragm actuator has been used in a microfluidic pump with its image shown in Fig. 6(b).[82] The microfluidic pump was made by integrating the unimorph diaphragm micro-actuator with a nozzle/diffuser to form a fluidic mechanical–diode structure. The flow rate increases linearly with frequency and reaches 25 mL/m (at 63 Hz with a back pressure of 350 Pa) for a 2 mm size pump. A simple analysis indicates that by increasing the diaphragm thickness and reducing the external fluid channel length, the operation frequency, as well as the pumping speed can be increased. The required voltage to drive the diaphragm actuator (under 71 MV/m) for desired performance can be significantly reduced by using multilayer configuration in which each electrostrictive layer thickness is in the range of 1 μm, as has been demonstrated by Choi et al. [Fig. 6(d)][83,84]

The electroactuation can be enhanced by introducing large dipole moment functional groups into a polymer that can be reoriented by external electric field. A P(VDF–TrEF) based electrostrictive graft elastomer (*G*-elastomer) was developed in 1999 by Su et al.,[85] showing high electrical field induced strain (~4%) and mechanical modulus (>750 MPa). Combination of these two essential properties makes the *G*-elastomer a promising electromechanically functional material for advanced actuators. A bi-layer actuator using *G*-elastomers has been developed,[86] offering bending actuation either in one direction or in two directions to meet the needs in applications. The bending actuation performance of the actuator has been evaluated in a benchtop wind tunnel for potential aerospace applications (such as morphing aircraft). Figure 6(c) presents the actuation performance of the bending actuators.

A core-free rolled actuator using P(VDF–TrFE–CFE) electrostrictive terpolymer thin film is another promising actuator example.[87] The actuator can generate up to 4% induced strain along the axial direction. For example, a 2.5 cm long actuator can generate 1 mm displacement. The size of the actuator is scalable based on the width and length of available films and the number of layers. One application of the cylinder actuators is for the refreshable Braille Display. By combinations of actuations from these actuators, the cell can display all the letters required for a Braille Display. Hence arranging these cells into a large assembly may realize a full page refreshable Braille Display or a Graphic Display, which will be extremely valuable for blind and visually impaired community.[87]

The application examples presented above show that the ferroelectric EAP actuators require a field of >50 MV/m to achieve significant electroactuation. For practical applications, the rational concerns are the applied voltage and the electric breakdown fields. Very high-voltage operation will increase the cost of the electronics and may limit the applications (for example, the operation voltage of mobile electronics and wearable devices should be low and in many cases, it is 40 V or below). To reduce the voltage required to drive the EAPs to achieve high electroactuation responses, thin EAP films in multilayer configuration are desired, since $E = V/d$ where V is the voltage and d is the thickness. On the other hand, thin EAP films, if the elastic modulus is low, will not generate much electroactuation if metal electrodes are used. The relative high elastic modulus (>0.5 GPa) of the ferroelectric relaxor polymer actuator films makes it possible to fabricate multilayer actuators with each layer thickness approaching 1 μm. For example, Choi et al. at Samsung Advanced Technology Institute developed a fabrication protocol to fabricate a P(VDF–TrFE–CTFE) multilayer electroactuation device with each polymer layer thickness about 1–1.5 μm, as shown in Fig. 6(d).[84] Such multilayer actuators have generated a large and fast strain response [inset of Fig. 6(e)] under a significant lowered voltage of 40 V which is in a safe voltage range for wearable and hand-held devices.[83] The multilayer actuators have been demonstrated to be very effective for varifocal microlens for smartphone cameras [see Fig. 6(e)]. In addition of making multilayer thin film to reduce applied voltage, great enhancement of permittivity could dramatically reduce the required electric field to generate large strains. PVDF polymer-based nanocomposites with appropriate fillers have been demonstrated to possess much larger dielectric constant compared with the PVDF neat polymer. The fillers are normally chosen from materials, which exhibit large dielectric constant or high electric conductivity, such as, copper phthalocyanine,[66] polyaniline particles,[88] and carbon nanotubes (CNTs).[89] Recently Javadi et al. reported a P(VDF–TrFE–CFE)/functionalized graphene nanosheets (FGNS) composites which exhibit giant dielectric constant,[90] where 4% strain was induced under

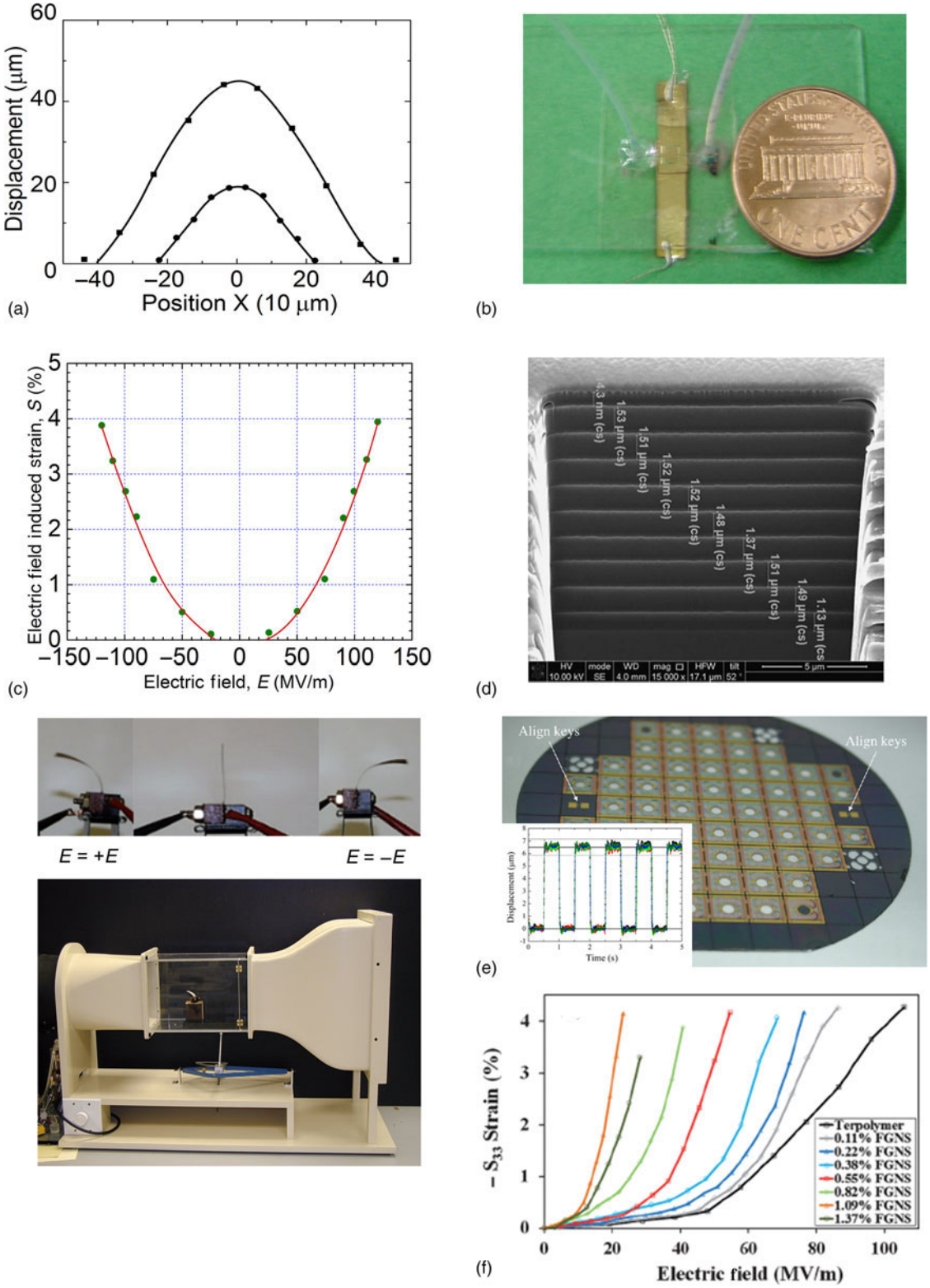

Figure 6. (a) Displacement versus position in a two end-supported unimorph diaphragm actuator utilizing an electrostrictive polymer. Reprinted with permission from Ref. 81. Copyright [2002], AIP Publishing LLC. (b) An image of a microfluidic pump. The figure is contributed by an author of this paper. (c) Actuation performance of the bending actuators in a bench-top wind tunnel. The figure is contributed by an author of this paper. (d) A P(VDF–TrFE–CFE) multilayer electroactuation device with each layer thickness about 1–1.5 μm. Reprinted from Ref. 84, Copyright (2013), with permission from Elsevier. (e) Displacement versus time (strain response) under 40 V voltage of the multilayer actuator. Adapted from Ref. 84, Copyright (2013), with permission from Elsevier (f) Strain versus electric field in P(VDF–TrFE–CFE)/FGNS composites. Reproduced from Ref. 90 with permission of The Royal Society of Chemistry.

an external electric field of about 20 MV/m, which is 5× reduction compared with pristine terpolymer as shown in Fig. 6(f).

Besides the electrostriction, the electrostatic forces generated from the interactions among the charges on the electrodes, as illustrated in Fig. 5, may also generate a large shape change in polymers. In the simplest form, the Maxwell stress-induced strain, similar to electrostriction, is also proportional to square of electric field, [Fig. 5(b)]. For an isotropic material, the strains are

$$x_3 = -\frac{\varepsilon_0 \kappa}{Y}\frac{1-2\nu}{2}E^2, \quad x_1 = \frac{\varepsilon_0 \kappa}{2Y}E^2, \tag{10}$$

where Y and ν are the Young's modulus and Poisson ratio, respectively, and κ is the permittivity.[91–97] Hence a dielectric with a low elastic modulus (for example, $Y \sim 1$ MPa) can generate significant electroactuations, as have been demonstrated in several dielectric elastomers which have a Yang's modulus ~1 MPa and a dielectric constant ~3, in which a Maxwell strain >100% has been achieved under an electric field >200 MV/m.

As we revisit Fig. 1(d), the ferroelectric relaxor polymer possesses a high dielectric constant at RT (>50), which is more than ten times higher than the most dielectric elastomers. However, the polymer does not generate much Maxwell stress-induced strain due to the high elastic modulus of the ferroelectric relaxor polymers, as can be deduced from Eq. (10). On the other hand, increasing the bulky ter-monomer such as CFE or CTFE in the ferroelectric relaxor polymers much beyond 10 mol% will cause a significant reduction of the elastic modulus. Such ferroelectric polymers may generate both large electrostriction and Maxwell stress-induced actuations and represent an interesting research direction for the development of the next generation of polymer actuator materials.

PVDF-based ferroelectric polymers for the capacitor applications

Compared with other types of capacitors, polymer film capacitors are inexpensive, easy to process, possess high dielectric strength, high-energy density and low dielectric loss, and fail gracefully. The state-of-the-art film DC bus capacitors, which use biaxially stretched polypropylene (BOPP) as the polymer dielectric, have low-energy density (<5 J/cm^3) caused by the low dielectric constant of 2.2.[19] Further increases of energy and power density in future dielectric materials are required by the demand for continuous miniaturization and increased functionality in modern electronics and electric power systems, since currently these capacitors contribute large (>30%) volume and weight to the whole systems (such as automotive inverters) because of the low-energy density.

The energy density U_e of the dielectric capacitors can be calculated with the equation: $U_e = \int E dD$, where E is the applied electric field and D is the electric polarization. For a linear dielectric, $D = \varepsilon_0 \kappa E$. As shown in Fig. 7(a), owing to the low dielectric constant ($\kappa = 2.2$), BOPP cannot reach a sufficiently large electric polarization to generate a large U_e, even under a field that is approaching its breakdown strength (>700 MV/m). Ferroelectric PVDF and P(VDF–TrFE) can achieve high electric polarization $P > 0.1$ C/m^2, which is still the highest in polymers, but high spontaneous polarization and ferroelectric hysteresis [Fig. 1(c)] prevent both energy storage and discharge in an effective manner, resulting in a minor improvement compared with

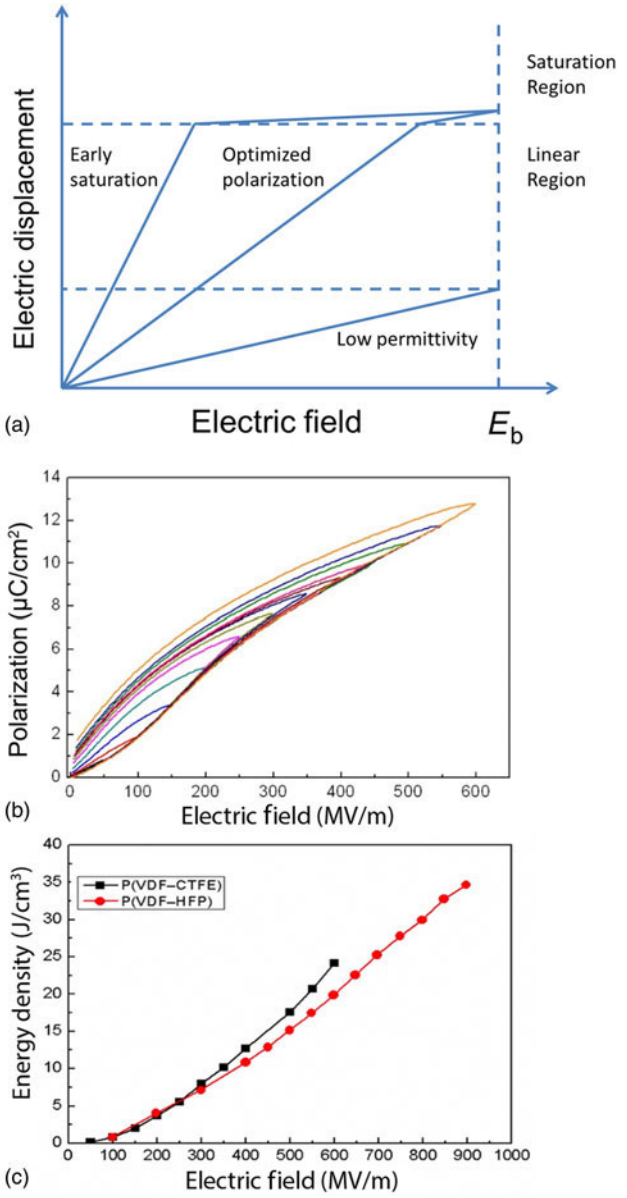

Figure 7. (a) Schematic illustration of the effect of dielectric constant K (the slope of D–E curve) on D_{sat} and energy density. A high K leads to the early D-saturation and consequently to a low-energy density. A low K leads to a low displacement and a low-energy density as well. An optimized dielectric constant K is able to achieve an optimized displacement and a high-energy density. (b) Unipolar polarization-electric field (D–E) loops of P(VDF–CTFE) with different maximum electric fields up to 600 MV/m under 10 Hz and RT. (c) Calculated discharge energy density of P(VDF–CTFE) and P(VDF–HFP) copolymers.

BOPP. As stated above, for electroactuation and EC functionalities, the issue is well addressed by the relaxor ferroelectric polymers. Treated by defect modulation, the relaxor ferroelectrics exhibit slim hysteresis loops that suggest much larger energy can be discharged and less energy dissipated than that of ferroelectric polymers. For example, in P(VDF–TrFE–CFE), which exhibits a large dielectric constant ($\kappa > 50$), discharge energy can reach 10 J/cm^3 which is 100% enhancement compared with ferroelectric P(VDF–TrFE).[20,98,99]

However, as shown in Fig. 7(a), high dielectric constant would induce a strong electric polarization response, which increases rapidly but saturate at a relatively low electric field, preventing energy density from growing at higher fields. Further increasing the applied field would only generate much smaller increment of electric polarization as the material entering the dielectric saturation region. It is important to recognize that the maximum stored energy density can be achieved by delicately modifying polymer's dielectric properties, i.e., a suitable dielectric constant, low ferroelectric and conduction loss, and high breakdown strength, as illustrated in Fig. 7.[20]

Above consideration is addressed by Chu et al. by investigating the P(VDF–CTFE) copolymer, in which the high concentration of bulky CTFE co-monomers results in not only a weaker ferroelectric hysteresis but also in the well-maintained dielectric constant ($K \sim 15$), thus allowing electric polarization growth in linear range until a high electric field is reached [Fig. 7(b)]. As a result, ultrahigh discharged energy density of 25 J/cm^3 can be achieved under $E = 600$ MV/m [Fig. 7(c)]. Similar D–E relationship was also discovered in the P(VDF-HFP) copolymer,[100] in which the discharged energy density can reach >30 J/cm^3 [Fig. 7(c)]. Compared with $U_e \sim$ 5 J/cm^3 from BOPP under 800 MV/m, U_e in those copolymers indicate a >4× improvement by introducing a desirable dielectric constant and high dielectric strength.

Short discharge time of capacitors (<1 μs) is highly desired in applications such as surgical lasers, high-power accelerators, and directed energy weapons.[101] Earlier studies reveal that both the P(VDF–TrFE–CFE) terpolymer and the P(VDF–CTFE) copolymer can achieve very fast discharge speeds,[20,21] due to the fast response of molecular dipoles exhibiting very little loss up to the MHz range.[21] As demonstrated using a capacitor discharge simulator, when the discharge time is reduced from >1 ms to <1 μs, the discharged energy density can be well-maintained at 60% of stored energy for P(VDF–CTFE). It is worthy to mention that, copolymer P(VDF–CTFE) and P(VDF–HFP) can be fabricated at a relatively low cost that is close to the cost of commercial PVDF.

Marked improvement in energy density and fast discharge time observed in PVDF-based ferroelectric polymers revealed great potential for high energy/power applications where compact, light-weighted capacitors are highly desirable. Besides ultrahigh energy density, it is important to reduce energy loss which will reduce efficiency and cause unwanted heating. Hysteresis loss can be directly estimated by the area that is enclosed in D–E loop as shown in Fig. 7(b), where about 30% of stored energy is lost owing to ferroelectric hysteresis. The hysteresis loss can be reduced by increasing the amount of CTFE or HFP which behave as a bulky defect modifiers. However, more "defects" would significantly reduce the elastic modulus of the polymer that is not desired for material processing and handling.

An encouraging strategy to suppress both dielectric loss and conduction loss is blending a polar polymer, which can reach high polarization but relatively large loss, with a non-polar polymer which has low dielectric constant but also possess much smaller losses. For instance, as observed by Wu et al. in P(VDF–CTFE)/ECTFE [P(ethylene-chlorotrifluoroethylene) (ECTFE)] blends,[102] hysteresis loss is successfully reduced by half (30 − 15%). The loss can be further reduced by crosslinking the blends, as shown in Fig. 8. Crosslinking in those blends hinders the polymer chain structures and prevents the formation of larger domains under high fields. As a result, the loss is limited

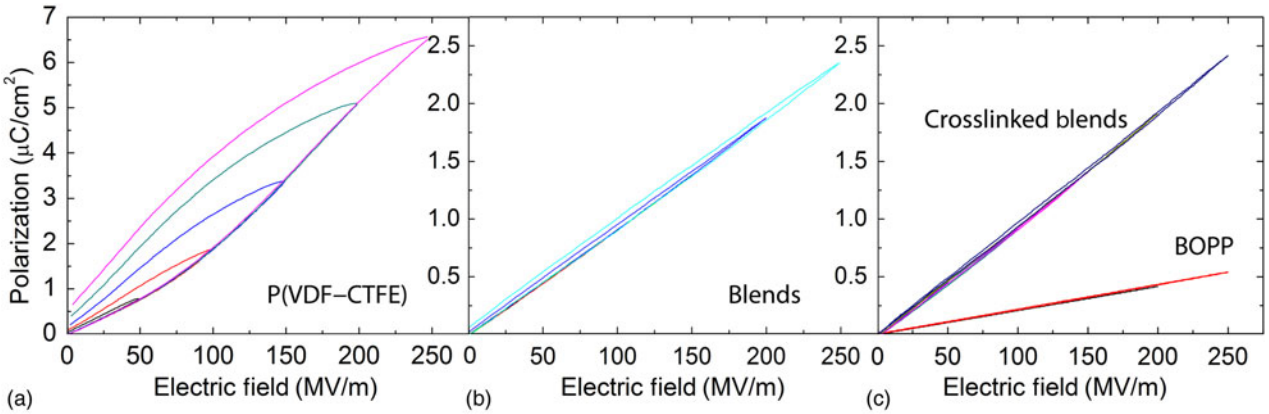

Figure 8. Polarization-electric field (D–E) responses under 10 Hz frequency at RT of (a) P(VDF–CTFE) 91/9 mol%, (b) P(VDF–CTFE)/ECTFE 67/33 wt% blends, and (c) P(VDF–CTFE)/ECTFE 67/33 wt% blends with chemical crosslinking under unipolar-electric fields. The D–E response of a commercial biaxially oriented polypropylene (BOPP) thin film is also presented in (c) for comparison. Reprinted with permission from Ref. 102. Copyright 2011, AIP Publishing LLC.

to below 5%, which is close to that of PP. Although the achieved energy density is far below the P(VDF–CTFE), the polarization of the blends is still 3× higher compared with PP.

In a neat ferroelectric polymer, electric polarization is primarily contributed by dipolar polarization. Further enhancement of polarization may be introduced by combining two or more materials to form a composite in which interfacial polarization can be contributing. Fabricating a nanocomposite containing nano-sized inorganic particles well dispersed in a polymer matrix is a general approach to maximize interfacial dielectric contribution. The dielectric responses of interfaces are critically dependent on charge/polarization distribution near the interfaces. When the nanocomposite is subjected to an electric field, interfaces are strongly modulated by local field fluctuations due to the contrast of dielectric/electric properties in participating components. Significant interfacial polarization can thus be introduced, crossing the double layers that form on both sides of interface region, as described in the composite model proposed by Tanaka et al.[103,104] The contrast between different components promotes both polarization and conduction processes. Strong local fields near interfaces may reduce the breakdown strength owing to the formation of percolated conduction channels when multiple interfacial double layers are overlapping. This is especially true when the nanofillers are highly conductive.

To prevent the formation of conduction channels, surface treatment of nano-fillers is proved to be a promising route by forming covalent bonding between the surface modifiers and nanoparticles.[105] As reported by Kim et al.,[106,107] phosphoric acid is demonstrated to be capable of forming covalent bonding with $BaTiO_3$ nanoparticles. Various functional groups thus could be selected to work with phosphoric acid to effectively improve the compatibility between the $BaTiO_3$ nanoparticle and different polymer matrixes. Hydroxyl group is another agent to induce covalent bonding to modify interfaces between the nanoparticles and polymer matrix. For instance, hydroxyl groups anchored on the surfaces of $BaTiO_3$ nanoparticles[108] or $Ba_{0.6}Sr_{0.4}TiO_3$ nanofibers[109] by peroxide treatment can form hydrogen bonds with the electrophilic atoms located on the polymer chains. Recently, dopamine, a bio-inspired building block used for interface modifications, has received considerable attention because of its unique structure containing both aromatic and amino groups, thus playing a role as a compatibilizer between the inorganic nanoparticle and polymer matrix.[110] Song et al.,[111] treated $BaTiO_3$ nanoparticles and nanofibers with dopamine in aqueous solutions. As a result, a ~5 nm thick dense layer is formed on the surface of the nanoparticles exhibiting high structural integrity and tight bonding between the nanoparticle and participating polymer. This layer not only promotes homogeneous dispersion of nanoparticles in host polymer, but also suppresses the remnant polarization usually associated with surface charges in the loose interfaces, leading to an enhancement of over 200% in the dielectric strength.

In addition to interface treatment, introducing large-aspect-ratio nanofillers in ferroelectric polymer matrix is proved to be effective to improve dielectric behavior. Low-dimensional nanofillers, such as nanofibers [one-dimensional (1D)], nano-sheets (2D), and aligned nano-particles, provide large dielectric anisotropy into the isotropic polymer matrix. Orienting those lower-dimension nanofillers along the external electric field direction would result in a high nanocomposite dielectric permittivity owing to the smaller depolarization factor and better penetration of electric field into the high permittivity inorganic fillers. For instance, nanocomposites containing highly oriented lead zirconium titanate (PZT) nanowires along the electric field exhibited >3× higher dielectric constant as compared with randomly filled nanocomposites.[112] On the other hand, orienting the fillers perpendicular to external electric field resulted in an improved dielectric strength.[113–115] In case of 2D nanosheets, when the longer dimension of the fillers is normal to the electric field, fillers form multiple energy barriers normal the field direction which increase the scattering of charged carriers and prevent forming of breakdown steamer tree. Additionally, high thermal conductivity and dielectric permittivity along the surface direction promotes the thermal and electric energy to dissipate in-plain and hence reduce the probability of breakdown along the field direction.[116–118] Most interestingly, it was recently reported that both enhancement of electrical polarization and dielectric strength can be achieved in a P(VDF–CTFE)-based ternary nanocomposite by adding high aspect ratio 2D hexagonal boron nitride nanosheets (12 wt%) and high permittivity $BaTiO_3$ nanoparticles (15 wt%) into P(VDF–CTFE), Li et al. observed a 20% increase in dielectric permittivity along with a 43% improvement in dielectric breakdown strength compared with pristine polymer matrix.[119] The addition of these nanoparticles also hindered the conversion of P(VDF–CTFE) polar phase, rendering a high charge–discharge efficiency of 82% even at the highest electrical field.

For a PVDF-based ferroelectric polymers and derived nanocomposites, it is worth noting that polymer fabrication processes can dramatically affect the dielectric properties and thus the energy storage performance. For instance, by quenching the PVDF-based nanocomposite thermally from 200 °C into ice water, weakly polar γ-phase in PVDF can be promoted along with the reduction of voids in the film. As a result, the nanocomposite exhibit slower polarization saturation behavior compared to what is normally observed in polar β-phase-dominated polymer matrix, without sacrificing the maximum polarization. Adding together, such processed nanocomposites show an ultrahigh energy density of 14.86 J/cm^3 at 450 MV/m and microsecond discharge time.[120]

Conclusions

PVDF-based ferroelectric EAPs provide unique soft material systems to explore dielectric, electromechanical, and electrothermal interactions among three major energy forms. Previous studies in electroactuation, ECE and high-energy density polymer capacitors demonstrated that by tailoring molecular, micro-, and meso-structure of a ferroelectric polymer,

energy conversion and storage in these soft materials can be specifically or concurrently improved. First, great ECE performance (30 K temperature change and over 50 °C temperature span including RT) has been achieved in relaxor ferroelectric polymers. By delicately modifying dipolar correlation to expand differences between dipolar-ordered and disordered phases, ECE is indeed improved. The giant ECE and wider operation temperature range near RT paves the way to new design of novel plastic coolers for efficient thermal management on different scales. Secondly, fast, large mechanic responses (>6% in strain) in relaxor ferroelectric terpolymer P(VDF-TrFE-CFE), which exhibit the highest dielectric constant among all pristine polymers, has been achieved under low electric field (20 MV/m) and safe voltage (40 V) in pristine polymer and its nanocomposites. The last but not the least, the energy density of the ferroelectric polymer-based dielectrics has reached more than 30 J/cm^3, which is at least 5× as high as for conventional polymer dielectrics. Optimized permittivity and modulated interfaces polarization not only enhanced the energy density that is stored in the polymer film but also offered modifications on multiple other material properties, i.e., dielectric strength, hysteresis/conduction loss, discharge time, etc.

Increasing knowledge and improvements of the electric-related responses of these ferroelectric polymers, along with the polymer's inherent compatibility with modern fabrication technologies such as 3D printing technology stimulate strong driving force to keep improving the soft materials to meet the ever increasing needs from practical applications and thus open new opportunities to develop novel stretchable, flexible and multifunctional machines and electroactive devices.

Acknowledgments

The research of ECE in modified ferroelectric PVDF-based polymers was supported by U.S. DoE, Office of Basic Energy Sciences, Division of Materials Science and Engineering under Award No. DE-FG02-07ER46410. The research of PVDF based polymers for capacitor application was supported by the Office of Naval Research, under grant No. N00014-14-1-0109.

References

1. J. Valasek: Piezo-electric and allied phenomena in Rochelle salt. *Phys. Rev.* **17**, 475 (1921).
2. M. Lines and A. Glass: *Principles and Applications of Ferroelectrics and Related Materials* (Larendon, Oxford, 1977).
3. H. Kawai: Piezoelectricity of poly (vinylidene fluoride). *Japan. J. Appl. Phys.* **8**, 975 (1969).
4. T.T. Wang, J.M. Herbert, and A.M. Glass: *The Applications of Ferroelectric Polymers* (Blackie; Chapman and Hall, Glasgow, New York, 1988).
5. G.M. Sessler: *Electrets* (Laplacian Press, Morgan Hill, CA., 1998).
6. Y. Xu: *Ferroelectric Materials and their Applications* (North-Holland; Sole distributors for the USA and Canada, Elsevier Science Pub. Co., Amsterdam, New York, NY, 1991).
7. A. Ambrosy and K. Holdik: Piezoelectric PVDF films as ultrasonic transducers. *J. Phys. E-Sci. Instrum.* **17**, 856 (1984).
8. V. Bhavanasi, D.Y. Kusuma, and P.S. Lee: Polarization orientation, piezoelectricity, and energy harvesting performance of ferroelectric PVDF–TrFE nanotubes synthesized by nanoconfinement. *Adv. Energy Mater.* **4**, 8 (2014).
9. R.B. Olsen, D.A. Bruno, and J.M. Briscoe: Pyroelectric conversion cycles. *J. Appl. Phys.* **58**, 4709 (1985).
10. L. Persano, C. Dagdeviren, Y. Su, Y. Zhang, S. Girardo, D. Pisignano, Y. Huang, and J.A. Rogers: High performance piezoelectric devices based on aligned arrays of nanofibers of poly(vinylidenefluoride-co-trifluoroethylene). *Nat. Commun.* **4**, 1633 (2013).
11. S.P. Alpay, J. Mantese, S. Trolier-McKinstry, Q. Zhang, and R.W. Whatmore: Next-generation electrocaloric and pyroelectric materials for solid-state electrothermal energy interconversion. *MRS Bull.* **39**, 1099 (2014).
12. R.C.G. Naber, K. Asadi, P.W.M. Blom, D.M. de Leeuw, and B. de Boer: Organic nonvolatile memory devices based on ferroelectricity. *Adv. Mater.* **22**, 933 (2010).
13. A.J. Lovinger: Ferroelectric polymers. *Science* **220**, 1115 (1983).
14. B. Neese, B. Chu, S.-G. Lu, Y. Wang, E. Furman, and Q.M. Zhang: Large electrocaloric effect in ferroelectric polymers near room temperature. *Science* **321**, 821 (2008).
15. S.-G. Lu and Q. Zhang: Electrocaloric materials for solid-state refrigeration. *Adv. Mater.* **21**, 1983 (2009).
16. X. Li, S.-G. Lu, X.-Z. Chen, H. Gu, X.-S. Qian, and Q.M. Zhang: Pyroelectric and electrocaloric materials. *J. Mater. Chem. C* **1**, 23 (2013).
17. Z. Cheng and Q. Zhang: Field-activated electroactive polymers. *MRS Bull.* **33**, 183 (2008).
18. W.J. Sarjeant, J. Zirnheld, and F.W. MacDougall: Capacitors. *IEEE Trans. Plasma Sci.* **26**, 1368 (1998).
19. M. Rabuffi and G. Picci: Status quo and future prospects for metallized polypropylene energy storage capacitors. *IEEE Trans. Plasma Sci.* **30**, 1939 (2002).
20. B.J. Chu, X. Zhou, K.L. Ren, B. Neese, M.R. Lin, Q. Wang, F. Bauer, and Q.M. Zhang: A dielectric polymer with high electric energy density and fast discharge speed. *Science* **313**, 334 (2006).
21. X. Zhou, Q. Chen, Q.M. Zhang, and S. Zhang: Dielectric behavior of bilayer films of P(VDF-CTFE) and low temperature PECVD fabricated Si3N4. *IEEE Trans. Dielectr. Electr. Insul.* **18**, 463 (2011).
22. Q.M. Zhang, J.G. Brisson II, J. Joe Smith, P. Calvert, F. Bauer, and G. Knowles: Relaxor ferroelectric polymer based electrotextile for thermal management of soldiers with protective gears, (Proposal Submitted to DARPA BAA 04-12 Addendum 7, 2004) http://www.ee.psu.edu/Directory/FacultyInfo/Zhang/ProposaldarpaSMFMNov1104%20-ECEPart.pdf
23. X. Li, X.-S. Qian, S.G. Lu, J. Cheng, Z. Fang, and Q.M. Zhang: Tunable temperature dependence of electrocaloric effect in ferroelectric relaxor poly(vinylidene fluoride-trifluoroethylene-chlorofluoroethylene terpolymer. *Appl. Phys. Lett.* **99**, 052907 (2011).
24. B. Li, W.J. Ren, X.W. Wang, H. Meng, X.G. Liu, Z.J. Wang, and Z.D. Zhang: Intrinsic electrocaloric effects in ferroelectric poly(vinylidene fluoride–trifluoroethylene) copolymers: roles of order of phase transition and stresses. *Appl. Phys. Lett.* **96**, 102903 (2010).
25. P.F. Liu, J.L. Wang, X.J. Meng, J. Yang, B. Dkhil, and J.H. Chu: Huge electrocaloric effect in Langmuir–Blodgett ferroelectric polymer thin films. *New J. Phys.* **12**, 023035 (2010).
26. B. Rozic, Z. Kutnjak, B. Neese, S.-G. Lu, and Q.M. Zhang: Electrocaloric effect in the relaxor ferroelectric polymer composition P(VDF-TrFE-CFE) 0.90-P(VDF-CTFE)0.10. *Phase Transit.* **83**, 819 (2010).
27. S.G. Lu, B. Rozic, Q.M. Zhang, Z. Kutnjak, and B. Neese: Enhanced electrocaloric effect in ferroelectric poly(vinylidene-fluoride/trifluoroethylene) 55/45 mol % copolymer at ferroelectric-paraelectric transition. *Appl. Phys. Lett.* **98**, 122906 (2011).
28. A.A. Skripkin, A.A. Solopov, A.V. Lyashenko, and A.A. Ignatyev: *High Frequency Air-cooling Radiator has Housing which has Input Portion that is made in Form of Venturi Nozzle, and has Inner Surface with thin Film Electrocaloric Polymer* (Tantal Stock Co; Inst Critical Technologies Stock Co; Univ Saratov) RU141660-U1.

29. V. Basso, F. Russo, J.-F. Gerard, and S. Pruvost: Direct measurement of the electrocaloric effect in poly(vinylidene fluoride-trifluoroethylene-chlorotrifluoroethylene) terpolymer films. *Appl. Phys. Lett.* **103**, 202904 (2013).
30. Y. Jia, and Y.S. Ju: Direct characterization of the electrocaloric effects in thin films supported on substrates. *Appl. Phys. Lett.* **103**, 042903 (2013).
31. R.L. Moreira: Electrocaloric effect in gamma-irradiated P(VDF–TrFE) copolymers with relaxor features. *Ferroelectrics* **446**, 1 (2013).
32. D. Guo, J. Gao, Y.-J. Yu, S. Santhanam, G.K. Fedder, A.J.H. McGaughey, and S.C. Yao: Electrocaloric characterization of a poly(vinylidene fluoride-trifluoroethylene-chlorofluoroethylene) terpolymer by infrared imaging. *Appl. Phys. Lett.* **105**, 031906 (2014).
33. Y. Jia, and Y.S. Ju: Characterization of the electrocaloric effect and hysteresis loss in relaxor ferroelectric thin films under alternating current bias fields. *Appl. Phys. Lett.* **104**, 251913 (2014).
34. X. Li, X.-S. Qian, H. Gu, X. Chen, S.G. Lu, M. Lin, F. Bateman, and Q.M. Zhang: Giant electrocaloric effect in ferroelectric poly (vinylidenefluoride-trifluoroethylene) copolymers near a first-order ferroelectric transition. *Appl. Phys. Lett.* **101**, 132903 (2012).
35. R. Pirc, Z. Kutnjak, R. Blinc, and Q.M. Zhang: Electrocaloric effect in relaxor ferroelectrics. *J. Appl. Phys.* **110**, 074113 (2011).
36. X. Li, X.-S. Qian, S.G. Lu, J. Cheng, Z. Fang, and Q.M. Zhang: Tunable temperature dependence of electrocaloric effect in ferroelectric relaxor poly(vinylidene fluoride-trifluoroethylene-chlorofluoroethylene terpolymer. *Appl. Phys. Lett.* **99**, 052907 (2011).
37. Z.K. Liu, X. Li, and Q.M. Zhang: Maximizing the number of coexisting phases near invariant critical points for giant electrocaloric and electromechanical responses in ferroelectrics. *Appl. Phys. Lett.* **101**, 082904 (2012).
38. X.-S. Qian, H.-J. Ye, Y.-T. Zhang, H. Gu, X. Li, C.A. Randall, and Q.M. Zhang: Giant electrocaloric response over a broad temperature range in modifi ed BaTiO 3 ceramics. *Adv. Funct. Mater.* **24**, 1300 (2014).
39. H.-J. Ye, X.-S. Qian, D.-Y. Jeong, S. Zhang, Y. Zhou, W.-Z. Shao, L. Zhen, and Q.M. Zhang: Giant electrocaloric effect in BaZr0.2Ti0.8O3 thick film. *Appl. Phys. Lett.* **105**, 152908 (2014).
40. X.-Z. Chen, X. Li, X.-S. Qian, M. Lin, S. Wu, Q.-D. Shen, and Q.M. Zhang: A nanocomposite approach to tailor electrocaloric effect in ferroelectric polymer. *Polymer* **54**, 5299 (2013).
41. G. Zhang, Q. Li, H. Gu, S. Jiang, K. Han, M.R. Gadinski, M.A. Haque, Q. Zhang, and Q. Wang: Ferroelectric polymer nanocomposites for room-temperature electrocaloric refrigeration. *Adv. Mater.* **27**, 1450 (2015).
42. H. Gu, X. Qian, X. Li, B. Craven, W. Zhu, A. Cheng, S.C. Yao, and Q.M. Zhang: A chip scale electrocaloric effect based cooling device. *Appl. Phys. Lett.* **102**, 122904 (2013).
43. H. Gu, X.-S. Qian, H.-J. Ye, and Q.M. Zhang: An electrocaloric refrigerator without external regenerator. *Appl. Phys. Lett.* **105**, 162905 (2014).
44. X.-Z. Chen, X.-S. Qian, X. Li, S.G. Lu, H.-m Gu, M. Lin, Q.-d Shen, and Q.M. Zhang: Enhanced electrocaloric effect in poly(vinylidene fluoride-trifluoroethylene)-based terpolymer/copolymer blends. *Appl. Phys. Lett.* **100**, 222902 (2012).
45. X.-Z. Chen, X. Li, X.-S. Qian, S. Wu, S.-G. Lu, H.-M. Gu, M. Lin, Q.-D. Shen, and Q.M. Zhang: A polymer blend approach to tailor the ferroelectric responses in P(VDF-TrFE) based copolymers. *Polymer* **54**, 2373 (2013).
46. H. Gu, X. Li, S.G. Lu, M. Lin, X. Qian, J.P. Cheng, Q.M. Zhang, A. Cheng and B. Craven: Compact cooling devices based on giant electrocaloric effect dielectrics. In *Proceedings of the Asme Summer Heat Transfer Conference, 2012, Vol 2*, 2012, p. 635.
47. H. Gu, X. Qian, X. Li, B. Craven, W. Zhu, A. Cheng, S.C. Yao, and Q.M. Zhang: A chip scale electrocaloric effect based cooling device. *Appl. Phys. Lett.* **102**, 122904 (2013).
48. H. Gu, B. Craven, X. Qian, X. Li, A. Cheng, and Q.M. Zhang: Simulation of chip-size electrocaloric refrigerator with high cooling-power density. *Appl. Phys. Lett.* **102**, 112901 (2013).
49. U. Plaznik, A. Kitanovski, B. Rozic, B. Malic, H. Ursic, S. Drnovsek, J. Cilensek, M. Vrabelj, A. Poredos, and Z. Kutnjak: Bulk relaxor ferroelectric ceramics as a working body for an electrocaloric cooling device. *Appl. Phys. Lett.* **106**, 043903 (2015).
50. R. Chukka, S. Shannigrahi, and L. Chen: Investigations of cooling efficiencies in solid-state electrocaloric device. *Integr. Ferroelectr.* **133**, 3 (2012).
51. Y.V. Sinyavsky and V.M. Brodyansky: Experimental testing of electrocaloric cooling with transparent ferroelectric ceramic as a working body. *Ferroelectrics* **131**, 321 (1992).
52. Y. Jia and Y. Sungtaek: A solid-state refrigerator based on the electrocaloric effect. *Appl. Phys. Lett.* **100**, 242901 (2012).
53. S.F. Karmanenko, O.V. Pakhomov, A.M. Prudan, A.S. Starkov, and A. Eskov: Layered ceramic structure based on the electrocaloric elements working as a solid state cooling line. *J. Eur. Ceram. Soc.* **27**, 3109 (2007).
54. M. Ozbolt, A. Kitanovski, J. Tusek, and A. Poredos: Electrocaloric refrigeration: thermodynamics, state of the art and future perspectives. *Int. J. Refrig. –Rev. Int. Froid* **40**, 174 (2014).
55. D. Guo, J. Gao, Y.-J. Yu, S. Santhanam, A. Slippey, G.K. Fedder, A.J.H. McGaughey, and S.-C. Yao: Design and modeling of a fluid-based micro-scale electrocaloric refrigeration system. *Int. J. Heat Mass Transfer* **72**, 559 (2014).
56. R.B. Olsen and D.D. Brown: High-efficiency direct conversion of heat to electrical energy-related pyroelectric measurements. *Ferroelectrics* **40**, 17 (1982).
57. Y.V. Sinyavsky, N.D. Pashkov, Y.M. Gorovoy, and G.E. Lugansky: The optical ferroelectric ceramic as working body for electrocaloric refrigeration. *Ferroelectrics* **90**, 213 (1989).
58. X.-S. Qian, S.-G. Lu, X. Li, H. Gu, L.-C. Chien, and Q. Zhang: Large electrocaloric effect in a dielectric liquid possessing a large dielectric anisotropy near the isotropic-nematic transition. *Adv. Funct. Mater.* **23**, 2894 (2013).
59. L. Zhu: Exploring strategies for high dielectric constant and low loss polymer dielectrics. *J. Phys. Chem. Lett.* **5**, 3677 (2014).
60. Y. Liu, J. Wei, P.-E. Janolin, I.C. Infante, X. Lou, and B. Dkhil: Giant room-temperature barocaloric effect and pressure-mediated electrocaloric effect in $BaTiO_3$ single crystal. *Appl. Phys. Lett.* **104**, 162904 (2014).
61. M. Redmond, K. Manickaraj, O. Sullivan, S. Mukhopadhyay, and S. Kumar: Hotspot cooling in stacked chips using thermoelectric coolers. *IEEE Trans. Compon. Packag. Manuf. Technol.* **3**, 759 (2013).
62. J.D. Jordan and J.R. Carhuapoma: Hypothermia: comparing technology. *J. Neurol. Sci.* **261**, 35 (2007).
63. A.J. Lovinger, T. Furukawa, G.T. Davis, and M.G. Broadhurst: Curie transitions in copolymers of vinylidene fluoride. *Ferroelectrics* **50**, 553 (1983).
64. A.J. Lovinger: Poly(Vinylidene Fluoride). In *Developments in Crystalline Polymers*, edited by D.C. Bassett (Applied Science Publishers, London, 1982), pp. 195–273.
65. C. Huang, R. Klein, F. Xia, H.F. Li, Q.M. Zhang, F. Bauer, and Z.Y. Cheng: Poly(vinylidene fluoride-trifluoroethylene) based high performance electroactive polymers. *Ieee Trans. Dielectr. Electr. Insulat.* **11**, 299 (2004).
66. Q.M. Zhang, V. Bharti, and X. Zhao: Giant electrostriction and relaxor ferroelectric behavior in electron-irradiated poly(vinylidene fluoride-trifluoroethylene) copolymer. *Science* **280**, 2101 (1998).
67. Z.Y. Cheng, T.B. Xu, V. Bharti, S.X. Wang, and Q.M. Zhang: Transverse strain responses in the electrostrictive poly(vinylidene fluoride-trifluorethylene) copolymer. *Appl. Phys. Lett.* **74**, 1901 (1999).
68. S.S. Guo, X.Z. Zhao, Q.F. Zhou, H.L.W. Chan, and C.L. Choy: High electrostriction and relaxor ferroelectric behavior in proton-irradiated poly (vinylidene fluoride-trifluoroethylene) copolymer. *Appl. Phys. Lett.* **84**, 3349 (2004).
69. F. Xia, Z.Y. Cheng, H.S. Xu, H.F. Li, Q.M. Zhang, G.J. Kavarnos, R.Y. Ting, G. Abdul-Sedat, and K.D. Belfield: High electromechanical responses in a poly(vinylidene fluoride-trifluoroethylene-chlorofluoroethylene) terpolymer. *Adv. Mater.* **14**, 1574 (2002).
70. H.S. Xu, Z.Y. Cheng, D. Olson, T. Mai, Q.M. Zhang, and G. Kavarnos: Ferroelectric and electromechanical properties of poly (vinylidene-fluoride-trifluoroethylene-chlorotrifluoroethylene) terpolymer. *Appl. Phys. Lett.* **78**, 2360 (2001).
71. J.T. Garrett, C.M. Roland, A. Petchsuk, and T.C. Chung: Electrostrictive behavior of poly(vinylidene fluoride-trifluoroethylene-chlorotrifluoroethylene). *Appl. Phys. Lett.* **83**, 1190 (2003).

72. Z.Y. Cheng, Q.M. Zhang, and F.B. Bateman: Dielectric relaxation behavior and its relation to microstructure in relaxor ferroelectric polymers: high-energy electron irradiated poly(vinylidene fluoride-trifluoroethylene) copolymers. *J. Appl. Phys.* **92**, 6749 (2002).
73. Z.Y. Cheng, D. Olson, H.S. Xu, F. Xia, J.S. Hundal, Q.M. Zhang, F.B. Bateman, G.J. Kavarnos, and T. Ramotowski: Structural changes and transitional behavior studied from both micro- and macroscale in the high-energy electron-irradiated poly(vinylidene fluoride-trifluoroethylene) copolymer. *Macromolecules* **35**, 664 (2002).
74. Z.M. Li, M.D. Arbatti, and Z.Y. Cheng: Recrystallization study of high-energy electron-irradiated P(VDF-TrFE) 65/35 copolymer. *Macromolecules* **37**, 79 (2004).
75. Z.M. Li, S.Q. Li, and Z.Y. Cheng: Crystalline structure and transition behavior of recrystallized-irradiated P(VDF-TrFE) 65/35 copolymer. *J. Appl. Phys.* **97**, 014102 (2005).
76. A.C. Jayasuriya, A. Schirokauer, and J.I. Scheinbeim: Crystal-structure dependence of electroactive properties in differently prepared poly(vinylidene fluoride/hexafluoropropylene) copolymer films. *J. Polym. Sci. B – Polym. Phys.* **39**, 2793 (2001).
77. M. Wegener, W. Kunstler, K. Richter, and R. Gerhard-Multhaupt: Ferroelectric polarization in stretched piezo- and pyroelectric poly(vinylidene fluoride-hexafluoropropylene) copolymer films. *J. Appl. Phys.* **92**, 7442 (2002).
78. B. Neese, Y. Wang, B. Chu, K. Ren, S. Liu, Q.M. Zhang, C. Huang, and J. West: Piezoelectric responses in poly(vinylidene fluoride/hexafluoropropylene) copolymers. *Appl. Phys. Lett.* **90**, 242917 (2007).
79. Z.M. Li, Y.H. Wang, and Z.Y. Cheng: Electromechanical properties of poly(vinylidene-fluoride-chlorotrifluoroethylene) copolymer. *Appl. Phys. Lett.* **88**, 062904 (2006).
80. R.J. Klein, F. Xia, Q.M. Zhang, and F. Bauer: Influence of composition on relaxor ferroelectric and electromechanical properties of poly(vinylidene fluoride-trifluoroethylene-chlorofluoroethylene). *J. Appl. Phys.* **97**, 094105 (2005).
81. T.B. Xu, Z.Y. Cheng, and Q.M. Zhang: High-performance micromachined unimorph actuators based on electrostrictive poly(vinylidene fluoride-trifluoroethylene) copolymer. *Appl. Phys. Lett.* **80**, 1082 (2002).
82. F. Xia, S. Tadigadapa, and Q.M. Zhang: Electroactive polymer based microfluidic pump. *Sens. Actuators a – Phys.* **125**, 346 (2006).
83. S.T. Choi, J.Y. Lee, J.O. Kwon, S. Lee, and W. Kim: Varifocal liquid-filled microlens operated by an electroactive polymer actuator. *Opt. Lett.* **36**, 1920 (2011).
84. S.T. Choi, J.O. Kwon, and F. Bauer: Multi layered relaxor ferroelectric polymer actuators for low-voltage operation fabricated with an adhesion-mediated film transfer technique. *Sens. Actuators a – Phys.* **203**, 282 (2013).
85. J. Su, J. Harrison, T. St Clair, J.S. Harrison, and T.L. St Clair: *Polymeric Piezoelectric Material* (Nasa Us Nat Aero & Space Admin; Nasa Us Nat Aero&Space Admin) WO200130875-A.
86. J. Su, J. Harrison, T. St Clair, J.S. Harrison, and T.L. St Clair: *Electromechanical Response Providing Device, has Active Web to Exhibit Electrostriction by Rotation of Polar Graft Moieties within Polymeric Web* (Nasa Us Nat Aero & Space Admin; Nasa Us Nat Aero&Space Admin) WO200131172-A.
87. T. Levard, P.J. Diglio, S.-G. Lu, C.D. Rahn, and Q.M. Zhang: Core-free rolled actuators for Braille displays using P(VDF–TrFE–CFE). *Smart Mater. Struct.* **21**, 012001 (2012).
88. C. Huang and Q.M. Zhang: Enhanced dielectric and electromechanical responses in high dielectric constant all-polymer percolative composites. *Adv. Funct. Mater.* **14**, 501 (2004).
89. S.H. Zhang, N.Y. Zhang, C. Huang, K.L. Ren, and Q.M. Zhang: Microstructure and electromechanical properties of carbon nanotube/poly(vinylidene fluoride-trifluoroethylene-chlorofluoroethylene) composites. *Adv. Mater.* **17**, 1897 (2005).
90. A. Javadi, Y. Xiao, W. Xu, and S. Gong: Chemically modified graphene/P(VDF-TrFE-CFE) electroactive polymer nanocomposites with superior electromechanical performance. *J. Mater. Chem.* **22**, 830 (2012).
91. R. Pelrine, R. Kornbluh, Q.B. Pei, and J. Joseph: High-speed electrically actuated elastomers with strain greater than 100%. *Science* **287**, 836 (2000).
92. M. Zhenyl, J.I. Scheinbeim, J.W. Lee, and B.A. Newman: High-field electrostrictive response of polymers. *J. Polym. Sci. B – Polym. Phys.* **32**, 2721 (1994).
93. G. Kofod, P. Sommer-Larsen, R. Kronbluh, and R. Pelrine: Actuation responsee of polyacrylate dielectric elastomers. *J. Intell. Mater. Syst. Struct.* **14**, 787 (2003).
94. Z.M. Li and Z.Y. Cheng: Partially ordered region—a new mechanism for electromechanical response of EAPs. In *Smart Structures and Materials 2005: Electroactive Polymer Actuators and Devices. Proceedings of SPIE* **5759**, 252 (2005).
95. X. Zhao and Z. Suo: Method to analyze electromechanical stability of dielectric elastomers. *Appl. Phys. Lett.* **91**, 061921 (2007).
96. G. Kofod, W. Wirges, M. Paajanen, and S. Bauer: Energy minimization for self-organized structure formation and actuation. *Appl. Phys. Lett.* **90**, 081916 (2007).
97. Q.M. Zhang, H.F. Li, M. Poh, F. Xia, Z.Y. Cheng, H.S. Xu, and C. Huang: An all-organic composite actuator material with a high dielectric constant. *Nature* **419**, 284 (2002).
98. L. Zhu and Q. Wang: Novel ferroelectric polymers for high energy density and low loss dielectrics. *Macromolecules* **45**, 2937 (2012).
99. S. Wu, M. Shao, Q. Burlingame, X. Chen, M. Lin, K. Xiao, and Q.M. Zhang: A high-K ferroelectric relaxor terpolymer as a gate dielectric for organic thin film transistors. *Appl. Phys. Lett.* **102**, 013301 (2013).
100. X. Zhou, X. Zhao, Z. Suo, C. Zou, J. Runt, S. Liu, S. Zhang, and Q.M. Zhang: Electrical breakdown and ultrahigh electrical energy density in poly(vinylidene fluoride-hexafluoropropylene) copolymer. *Appl. Phys. Lett.* **94**, 162901 (2009).
101. D.C. Bassett: *Developments in Crystalline Polymers—1* (Applied Science Publishers, London, 1982).
102. S. Wu, M. Lin, S.G. Lu, L. Zhu, and Q.M. Zhang: Polar-fluoropolymer blends with tailored nanostructures for high energy density low loss capacitor applications. *Appl. Phys. Lett.* **99**, 132901 (2011).
103. T. Tanaka, M. Kozako, N. Fuse, and Y. Ohki: Proposal of a multi-core model for polymer nanocomposite dielectrics. *IEEE Trans. Dielectr. Electr. Insul.* **12**, 669 (2005).
104. T.J. Lewis: Interfaces are the dominant feature of dielectrics at the nanometric level. *IEEE Trans. Dielectr. Electr. Insul.* **11**, 739 (2004).
105. Y. Rao and C.P. Wong: Material characterization of a high-dielectric-constant polymer-ceramic composite for embedded capacitor for RF applications. *J. Appl. Polym. Sci.* **92**, 2228 (2004).
106. P. Kim, N.M. Doss, J.P. Tillotson, P.J. Hotchkiss, M.-J. Pan, S.R. Marder, J. Li, J.P. Calame, and J.W. Perry: High energy density nanocomposites based on surface-modified $BaTiO_3$ and a ferroelectric polymer. *ACS Nano* **3**, 2581 (2009).
107. P. Kim, S.C. Jones, P.J. Hotchkiss, J.N. Haddock, B. Kippelen, S.R. Marder, and J.W. Perry: Phosphonic acid-modiried barium titanate polymer nanocomposites with high permittivity and dielectric strength. *Adv. Mater.* **19**, 1001 (2007).
108. T. Zhou, J.-W. Zha, R.-Y. Cui, B.-H. Fan, J.-K. Yuan, and Z.-M. Dang: Improving dielectric properties of $BaTiO_3$/ferroelectric polymer composites by employing surface hydroxylated $BaTiO_3$ nanoparticles. *ACS Appl. Mater. Interfaces* **3**, 2184 (2011).
109. S. Liu, J. Zhai, J. Wang, S. Xue, and W. Zhang: Enhanced energy storage density in poly(vinylidene fluoride) nanocomposites by a small loading of suface-hydroxylated $Ba_{0.6}Sr_{0.4}TiO_3$ nanofibers. *ACS Appl. Mater. Interfaces* **6**, 1533 (2014).
110. H. Lee, S.M. Dellatore, W.M. Miller, and P.B. Messersmith: Mussel-inspired surface chemistry for multifunctional coatings. *Science* **318**, 426 (2007).
111. Y. Song, Y. Shen, H. Liu, Y. Lin, M. Li, and C.-W. Nan: Improving the dielectric constants and breakdown strength of polymer composites: effects of the shape of the $BaTiO_3$ nanoinclusions, surface modification and polymer matrix. *J. Mater. Chem.* **22**, 16491 (2012).
112. H. Tang, Y. Lin, and H.A. Sodano: Enhanced energy storage in nanocomposite capacitors through aligned PZT nanowires by uniaxial strain assembly. *Adv. Energy Mater.* **2**, 469 (2012).
113. Y.U. Wang and D.Q. Tan: Computational study of filler microstructure and effective property relations in dielectric composites. *J. Appl. Phys.* **109**, 104102 (2011).

114. Y.U. Wang, D.Q. Tan, and J. Krahn: Computational study of dielectric composites with core–shell filler particles. *J. Appl. Phys.* **110**, 044103 (2011).
115. V. Tomer and C.A. Randall: High field dielectric properties of anisotropic polymer–ceramic composites. *J. Appl. Phys.* **104**, 074106 (2008).
116. S. Boggs: Analytical approach to breakdown under impulse conditions. *IEEE Trans. Dielectr. Electr. Insul.* **11**, 90 (2004).
117. R. Vogelsang, T. Farr, and K. Frohlich: The effect of barriers on electrical tree propagation in composite insulation materials. *IEEE Trans. Dielectr. Electr. Insul.* **13**, 373 (2006).
118. S.M. Lebedev, O.S. Gefle, and Y.P. Pokholkov: The barrier effect in dielectrics: the role of interfaces in the breakdown of inhomogeneous dielectrics. *IEEE Trans. Dielectr. Electr. Insul.* **12**, 537 (2005).
119. Q. Li, K. Han, M.R. Gadinski, G. Zhang, and Q. Wang: High energy and power density capacitors from solution-processed ternary ferroelectric polymer nanocomposites. *Adv. Mater.* **26**, 6244 (2014).
120. W. Li, Q. Meng, Y. Zheng, Z. Zhang, W. Xia, and Z. Xu: Electric energy storage properties of poly(vinylidene fluoride). *Appl. Phys. Lett.* **96**, 192905 (2010).